Supplemental Information

Phase Behavior and Superprotonic Conductivity in the System (1-*x*)CsH_2PO_4 – *x*H_3PO_4: Discovery of Off-stoichiometric α-[$Cs_{1-x}H_x$]H_2PO_4

Louis S. Wang,[†] Sawankumar V. Patel,[‡] Erica Truong,[‡] Yan-Yan Hu,[‡,ŧ] Sossina M. Haile[†,ϕ,*]

† Materials Science & Engineering, Northwestern University, 2220 Campus Drive, Evanston, Illinois 60208, United States

‡ Department of Chemistry & Biochemistry, Florida State University, 95 Chieftan Way, Tallahassee, Florida 32306, United States

ϕ Applied Physics, Northwestern University, 2220 Campus Drive, Evanston, Illinois 60208, United States

ŧ Center of Interdisciplinary Magnetic Resonance, National High Magnetic Field Laboratory, 1800 East Paul Dirac Drive, Tallahassee, Florida 32310, United States

Figure S1. Comparison of X-ray diffraction patterns and refinement results obtained from the (1-x)CsH_2PO_4-xH_3PO_4 material of global composition x = 0.07, before and after annealing at 230 °C (under pH_2O = 0.4 atm) for 3 days. Post-annealing data collected after 6 days at ambient temperature, and both measurements are obtained from well-ground samples. The refined phase weight fractions of CDP(m) and $CsH_5(PO_4)_2$ are within error of the input values of 0.893 and 0.107 weight fractions, respectively. All structure parameters of CDP(m) (space group $P2_1/m$), except lattice parameters, were fixed to those reported by Matsunaga *et al.*[1] (including anisotropic displacement parameters and hydrogen positions), whereas the model for $CsH_5(PO_4)_2$ (space group $P2_1/c$) was taken from that reported by Efremov *et al.*[2] (including hydrogen positions). For the latter phase, displacement parameters for all atoms were set to 0.01 Å^{-2}. All structure parameters except lattice parameters were fixed during refinement. Default GSAS-II peak profiles were employed (*i.e.*, the peaks were modeled as pseudo-Voigt functions), and the broadening was entirely attributed to the instrument. The 5 profile parameters and their Θ-dependences were established from a measurement using a LaB_6 standard (NIST SRM 660c) and were fixed during refinement. Each background was treated with a (unique) Chebyshev polynomial with 10 coefficients. In the final analysis cycle, lattice parameters and sample displacement parameter were refined. The results show that under conditions promoting equilibration, the phase transitions on heating that yield α-CDP are fully reversible.

Pre-anneal, R_{wp} = 8.78 %	a (Å)	b (Å)	c (Å)	β (°)	wt. frac.	expected
CDP(m)	7.902(2)	6.3813(2)	4.8735(8)	107.697(3)	0.887(2)	0.893
$CsH_5(PO_4)_2$	10.871(4)	7.761(2)	9.524(4)	96.67(2)	0.115(4)	0.107
Post-anneal, R_{wp} = 7.50 %	a (Å)	b (Å)	c (Å)	β (°)	wt. frac.	expected
CDP(m)	7.904(2)	6.3832(2)	4.8753(6)	107.702(3)	0.903(2)	0.893
$CsH_5(PO_4)_2$	10.874(4)	7.764(2)	9.519(4)	96.62(3)	0.097(4)	0.107

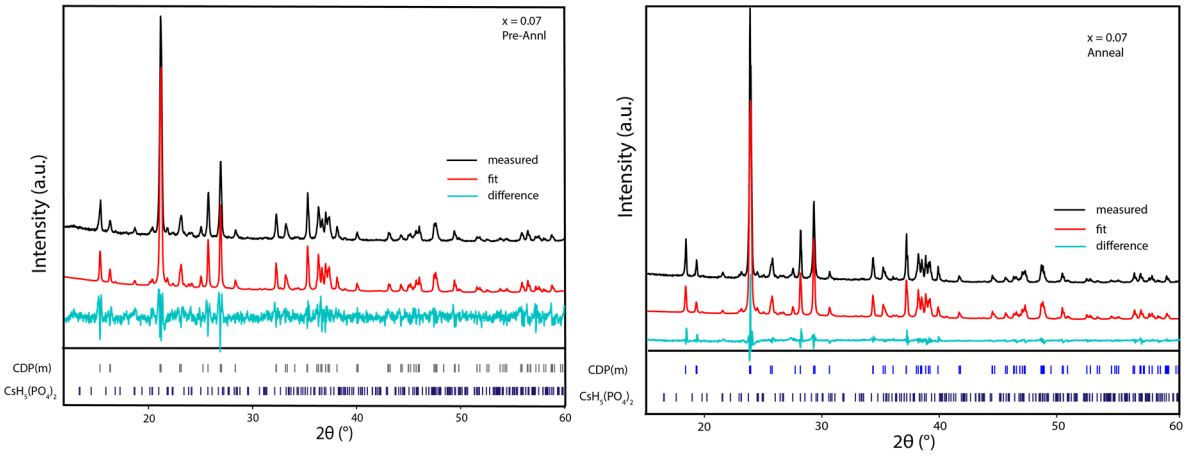

Figure S2. Comparison of differential scanning calorimetry and differential thermogravimetric profiles for samples in the (1-*x*)CsH_2PO_4-*x*H_3PO_4 system with global composition as indicated. In all cases, mass loss occurs at temperatures beyond the phase transitions of CPP formation and α-CDP(ss) formation detected by calorimetry.

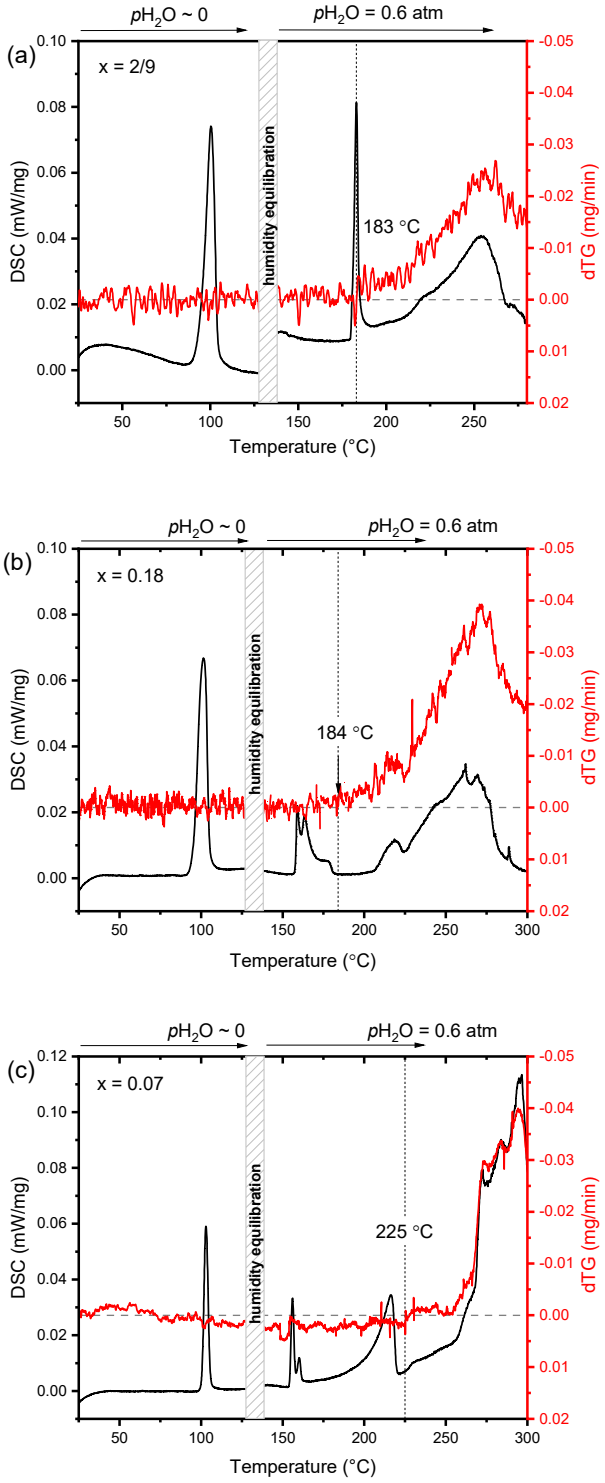

Figure S3. Thermal analysis of the (1-*x*)CsH_2PO_4-*x*H_3PO_4 material of global composition *x* = 0.15: (a) DSC and TG profiles; and (b) DSC and dTG profiles. Formation of CPP initiates at 96.5 °C, whereas formation of α-CDP(ss) initiates at 154.6 °C. Dehydration under these conditions of pH_2O = 0.4 atm initiates at 178 °C, well past the temperatures at which CPP and α-CDP(ss) form.

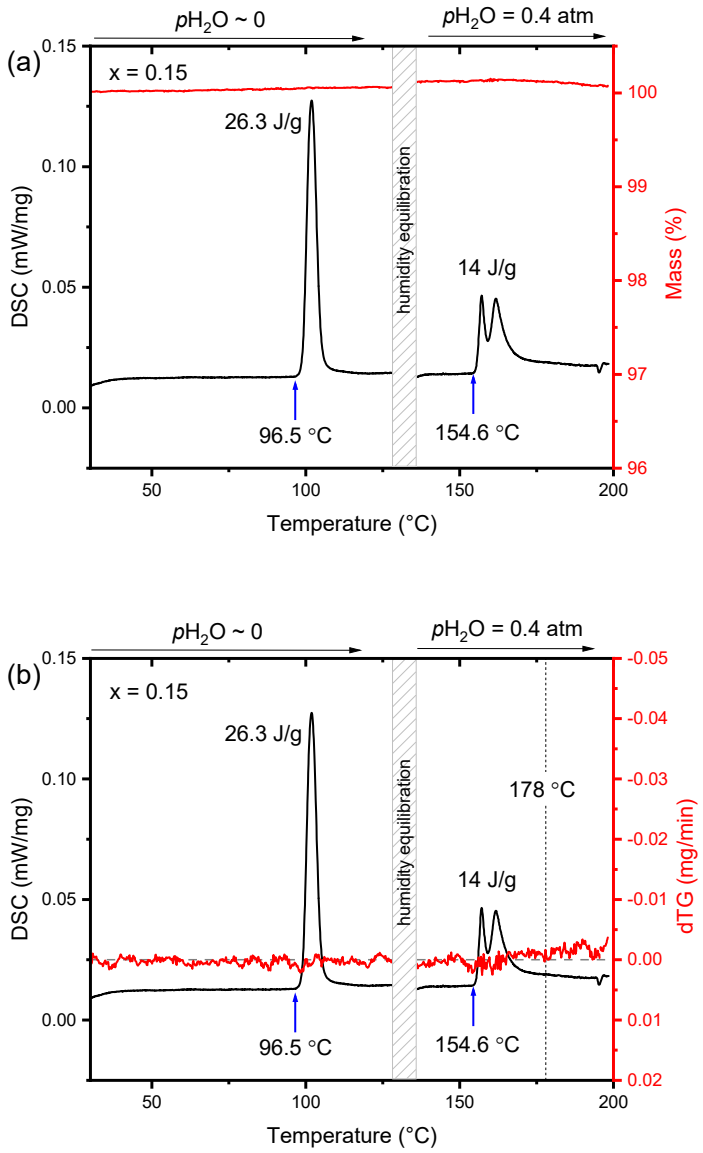

Figure S4. Example results of Rietveld refinement against diffraction data from the (1-*x*)CsH_2PO_4-*x*H_3PO_4 material of global composition *x* = 2/9 for selected temperatures (110 °C, CPP phase; and 180 °C, α-CDP(ss) phase), and accompanying listing of lattice parameter at each measurement/refinement temperature. Patterns shown correspond to those of main text Figure 2b. In the temperature range 110-170 °C, all structure parameters of CPP except lattice parameter and hydrogen positions were fixed to those reported in Wang *et al*.[3] (including anisotropic displacement parameters). The structure (space group *Pm*-3*n*) has 29 non-hydrogen atom positions in the asymmetric unit with all oxygen atoms sitting on sites of one-third occupancy. In the temperature range 180-186 °C, all non-hydrogen atomic positions were fixed to those reported by Yamada *et al*.[4] for the structure of cubic CDP (space group *Pm*-3*m*) and displacement factors treated as isotropic, with a fixed U_{iso} of 0.01 $Å^{-2}$. The structure has 3 non-hydrogen atom positions in the asymmetric unit with the single, crystallographically distinct oxygen atom sitting on a site of one-sixth occupancy. Although, as shown in this work, Cs vacancies occur in α-CDP this feature was not modeled in the refinement. Hydrogen atoms were omitted from both structure models. Default GSAS-II peak profiles were employed (*i.e.*, the peaks were modeled as pseudo-Voigt functions), and the broadening was entirely attributed to the instrument. The 5 profile parameters and their Θ-dependences were established from a measurement using a LaB_6 standard (NIST SRM 660c), which were then held fixed during refinement. Each background was treated with a (unique) Chebyshev polynomial with 10 coefficients. The sample displacement was treated in the following way. At the measurement temperature of 100 °C, at which CPP was fully formed, lattice parameter and sample displacement were simultaneously refined. Sample displacement was then held fixed for subsequent refinements involving the CPP structure. Similarly, the lattice parameter of α-CDP and the sample displacement were simultaneously refined at 180 °C, and the latter held fixed at this new value for all higher temperature refinements. Preferred orientation in α-CDP was treated (though not adequately captured) using an 8th order spherical harmonic model. In the final analysis cycle for each measurement temperature, only the lattice parameter was refined.

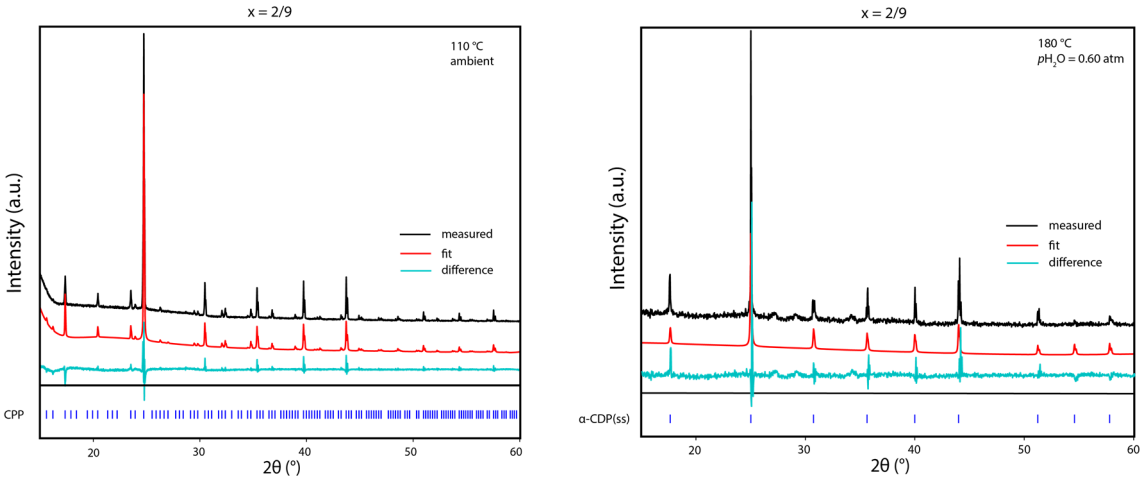

Figure S4. Continued.

Temperature (°C)	CPP *a*, (Å)	R_{wp}, %
100	20.1783(3)	8.63
105	20.1807(3)	8.56
110	20.1850(2)	8.14
110	20.1860(3)	8.54
115	20.1886(3)	8.34
115	20.1886(3)	8.34
120	20.1929(2)	7.78
120	20.1940(3)	8.36
125	20.1963(3)	8.31
130	20.2032(2)	7.60
130	20.2004(3)	8.19
135	20.2047(3)	8.14
140	20.2105(2)	7.69
140	20.2093(3)	7.92
170	20.231(3)	12.66

Temperature (°C)	α-CDP *a*, (Å)	$R_{wp,}$ %
180	5.0457(3)	15.72
180	5.0446(7)	10.33
182	5.0451(9)	11.40
184	5.0461(9)	11.09
186	5.0466(8)	10.71

Figure S5. Example results of Rietveld refinement against diffraction data from the (1-x)CsH_2PO_4-xH_3PO_4 material of global composition x = 0.18 at 140 and 160 °C, and accompanying listing of lattice parameter at each measurement/refinement temperature. Patterns shown correspond to main text Figure 3b. At 140 °C the phases CDP(m) and CPP are present. All structure parameters of CDP(m), except lattice parameters, were fixed to those reported by Matsunaga *et al.*[1] (including anisotropic displacement parameters and hydrogen positions), whereas all structure parameters of CPP, except lattice parameter, were fixed to those reported in Wang *et al.*[3] (including anisotropic displacement parameters). The structure of CDP(m) has 5 non-hydrogen atoms in the asymmetric unit, with all (non-hydrogen) sites fully occupied. The structure of CPP has 29 atom positions in the asymmetric unit with all oxygen atoms sitting on sites of one-third occupancy. At 160 °C and higher, only α-CDP is present. The atomic positions in this phase were fixed to those reported by Yamada *et al.*[3] for the structure of cubic CDP and displacement factors treated as isotropic, with a fixed U_{iso} of 0.01 $Å^{-2}$. The structure has 3 non-hydrogen atom positions in the asymmetric unit with the single, crystallographically distinct oxygen atom sitting on a site of one-sixth occupancy. Although, as shown in this work, Cs vacancies occur in α-CDP this feature was not modeled in the refinement. Hydrogen atoms were omitted from structure models of CPP and α-CDP. Default GSAS-II peak profiles were employed (*i.e.*, the peaks were modeled as pseudo-Voigt functions), and the broadening was entirely attributed to the instrument. The 5 profile parameters and their Θ-dependences were established from a measurement using a LaB_6 standard (NIST SRM 660c), which were then held fixed during refinement. Each background was treated with a (unique) Chebyshev polynomial with 10 coefficients. The sample displacement was treated in the following way. At 140 °C, at which CPP is the dominant phase, sample displacement and CPP lattice parameter were refined simultaneously. Displacement was then fixed, and lattice parameters of both CDP(m) and CPP refined, along with phase fraction. At 160 °C, at which α-CDP was fully formed, lattice parameter and sample displacement were simultaneously refined. Sample displacement was then held fixed for subsequent refinements involving the α-CDP structure. Preferred orientation in α-CDP was treated (though not adequately captured) using an 8th order spherical harmonic model.

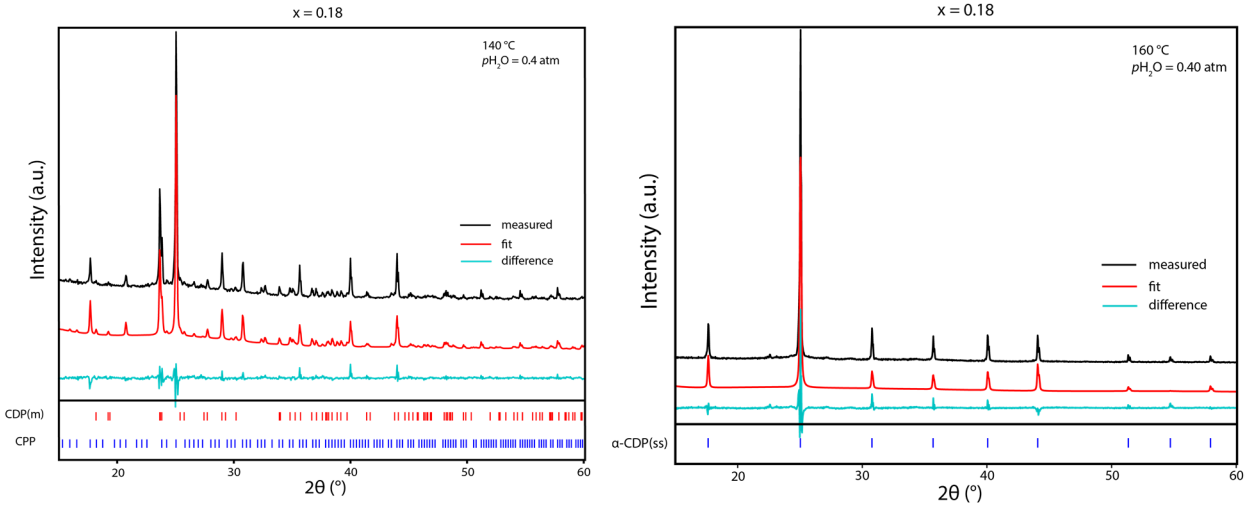

Figure S5. Continued

T (°C)	Monoclinic CDP lattice parameters				CPP *a*, (Å)	Wt. Frac. CPP	R_{wp}
	a (Å)	b (Å)	c (Å)	β (°)	a (Å)		
140	7.916(6)	6.463(1)	4.863(2)	107.12(1)	20.2153(8)	0.781(5)	8.24

Temperature (°C)	α-CDP *a*, (Å)	R_{wp} %
160	5.0298(4)	14.67
162	5.0282(2)	14.93
165	5.0290(2)	14.45
167	5.0296(2)	13.69
170	5.0309(2)	13.45
172	5.0317(2)	13.56
174	5.0325(2)	13.32
176	5.0329(2)	13.30

Figure S6. Zoomed in presentations of the (a) ^{31}P and (b) ^{1}H NMR spectra collected from the (1-*x*)CsH_2PO_4-*x*H_3PO_4 material of global composition *x* = 0.18 (eutectoid composition) at the indicated temperatures, which lie below the eutectoid reaction temperature. Highlighted regions show the signal from the CDP(m) phase.

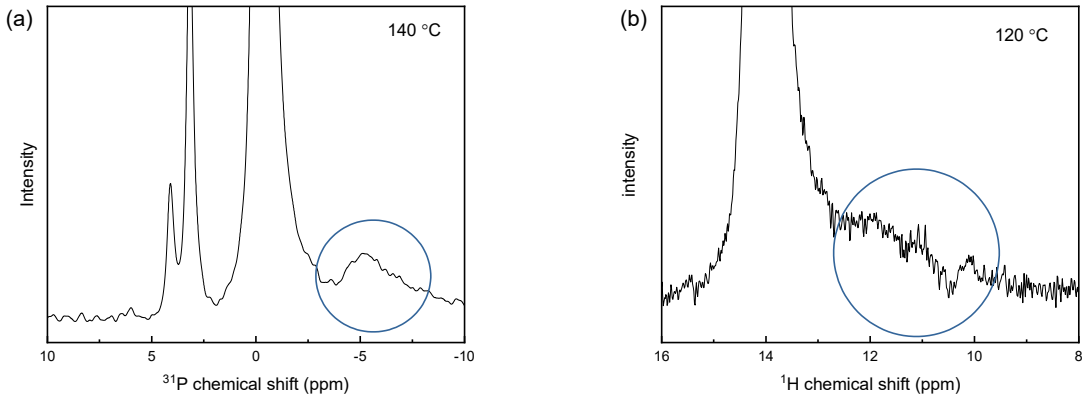

Figure S7. Deconvolution of the (a) ^{1}H and (b) ^{31}P NMR resonances collected from the (1-*x*)CsH_2PO_4-*x*H_3PO_4 material of global composition *x* = 0.18 (eutectoid composition) at the indicated temperatures.

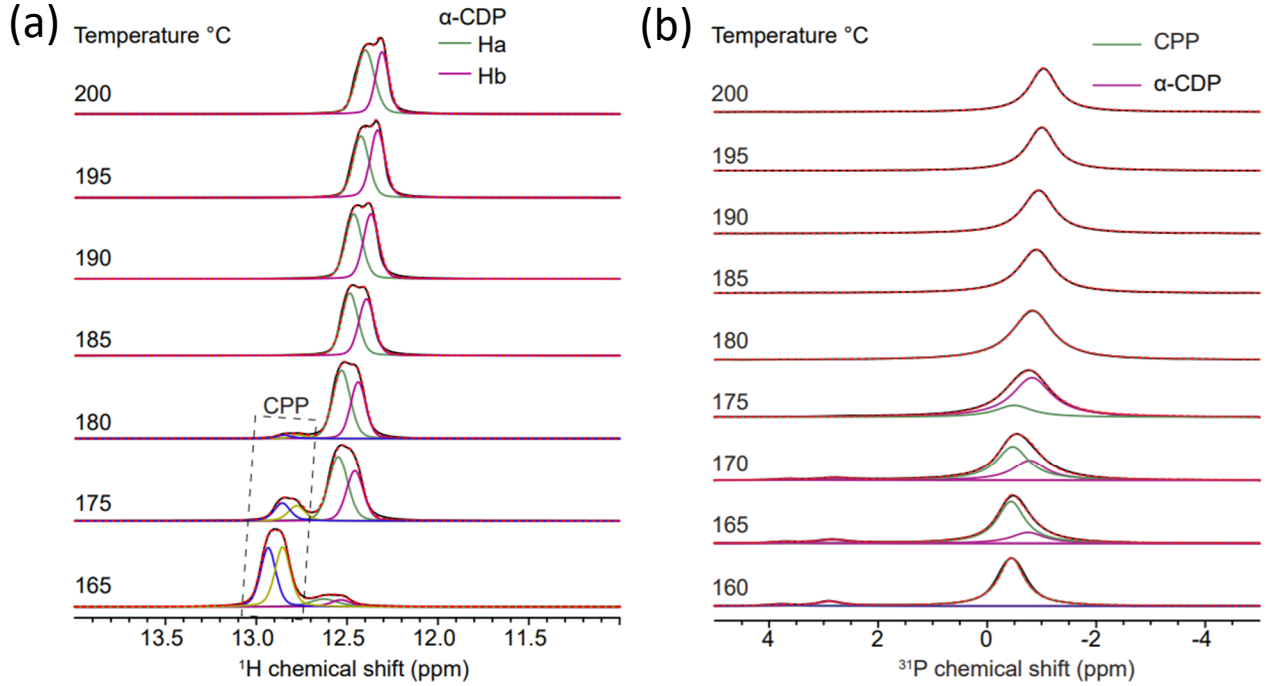

Figure S8. Example results of Rietveld refinement against diffraction data from the (1-*x*)CsH_2PO_4-*x*H_3PO_4 material of global composition *x* = 0.07 (data correspond to main text Figure 6b). Refinement procedures followed the methodology described above in the descriptions of Figures S1, S4, and S5. With the exception of lattice parameters, the structure of CDP(m) was fixed to that reported by Matsunaga *et al.*[1] and the structure of CPP to that reported by Wang *et al*.[3] The structure of α-CDP was modeled according to that reported by Yamada *et al*.[4] for cubic CDP. Although, as shown in this work, Cs vacancies occur in α-CDP, Cs site occupancy was fixed at 1. In addition to lattice parameter, isotropic displacement parameters were refined for α-CDP. At temperatures at which more than one phase appeared in the pattern, phase fractions were also refined. Peak profiles were modeled with pseudo-Voigt functions using fixed parameters determined from a separate measurement using a LaB_6 standard (NIST SRM 660c). Each background was treated with a (unique) Chebyshev polynomial with 10 coefficients.

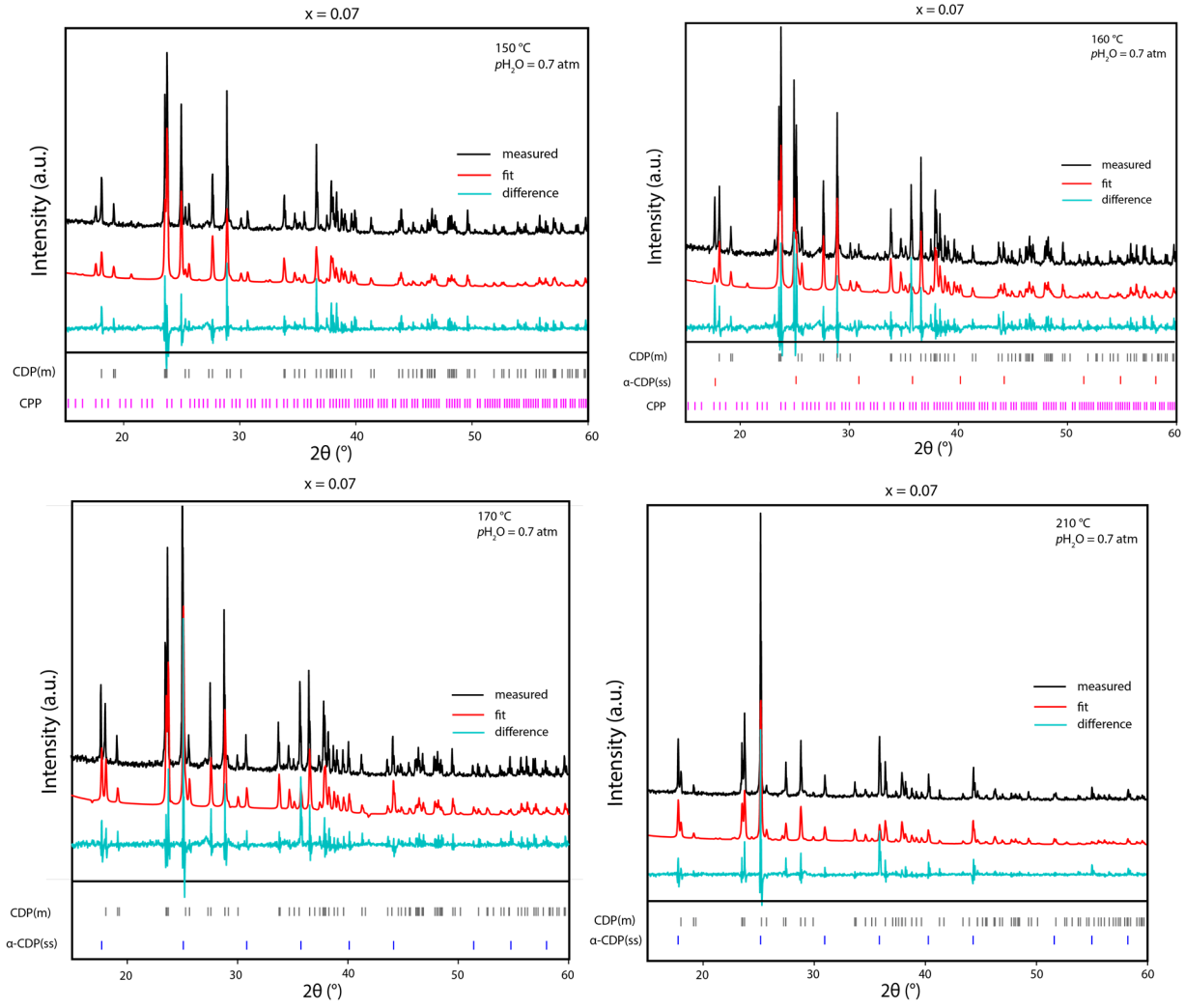

Figure S8. Continued.

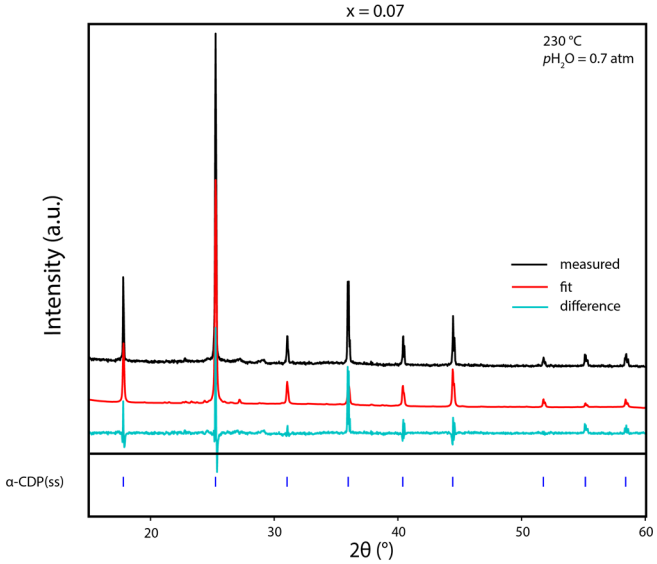

(°C)	Monoclinic CDP				CPP	α-CDP	R_{wp}, %
	a (Å)	*b* (Å)	*c* (Å)	β (°)	*a* (Å)	*a* (Å)	
150	7.924(5)	6.4621(8)	4.866(2)	107.179(9)	20.217(4)	N/A	18.47
160	7.921(4)	6.4681(5)	4.864(1)	107.128(8)	20.220(4)	5.0206(8)	20.10
170	7.924(4)	6.4755(6)	4.863(2)	107.082(9)	N/A	5.0281(4)	18.63
210	7.927(5)	6.5115(9)	4.856(2)	106.82(1)	N/A	5.0114(4)	18.55
230	N/A	N/A	N/A	N/A	N/A	4.9961(3)	19.62

Figure S9. Cell volumes of (a) CCP and (b) CDP(m) as functions of temperature. Equivalence of values from single phase and mixed phase materials reveals the fixed stoichiometric nature of these compounds. Results obtained from Rietveld refinement as described in the heading to Figure S10.

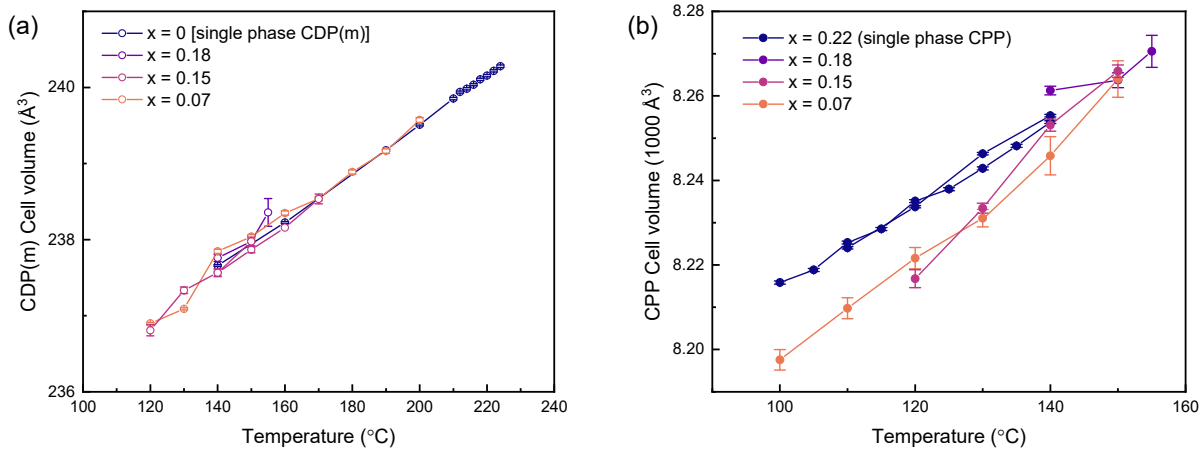

Figure S10. Temperature dependence of lattice constant and phase fraction of α-CDP(ss) component in samples of various compositions (as indicated) in the (1-*x*)CsH_2PO_4-*x*H_3PO_4 system (a-d), and (e) lattice expansion behavior in the single phase region. The average expansion of 2.2(1) × 10^{-4} Å/ °C was used in the evaluation of the solvus phase boundary. Complete listing of results obtained by Rietveld analysis of the corresponding diffraction patterns is also provided. Uncertainties in lattice parameters and phase fractions fall within the span of the symbols used to plot the data. Refinement procedures followed the methodology reported above in the description of Figure S8. In the two-phase regions, the structure of CDP(m) was fixed, with the exception of lattice parameters, to that reported by Matsunaga *et al.*[1] The structure of α-CDP was modeled according to the report by Yamada *et al.*[4] for cubic CDP. Although, as shown in this work, Cs vacancies occur in α-CDP, Cs site occupancy was fixed at 1. In addition to lattice parameter, isotropic displacement parameters were refined for α-CDP. At temperatures at which more than one phase appeared in the pattern, phase fractions were also refined. Peak profiles were modeled with pseudo-Voigt functions using fixed parameters determined from a separate measurement using a LaB_6 standard (NIST SRM 660c). Each background was treated with a (unique) Chebyshev polynomial with 10 coefficients. The sample displacement was treated in the following way. At 160 °C, at which CPP is the dominant phase, sample displacement and CPP lattice parameter were refined simultaneously. Displacement was then fixed, and lattice parameters of both CDP(m) and CPP refined, along with phase ratio. At 160 °C, at which CDP(m) was the dominant phase, the lattice parameters of this structure and the sample displacement were simultaneously refined. Sample displacement was then held fixed for subsequent refinements for a global given composition. Lines in between points in the figures serve only to guide the eye and do not reflect sample behavior between measurement temperatures.

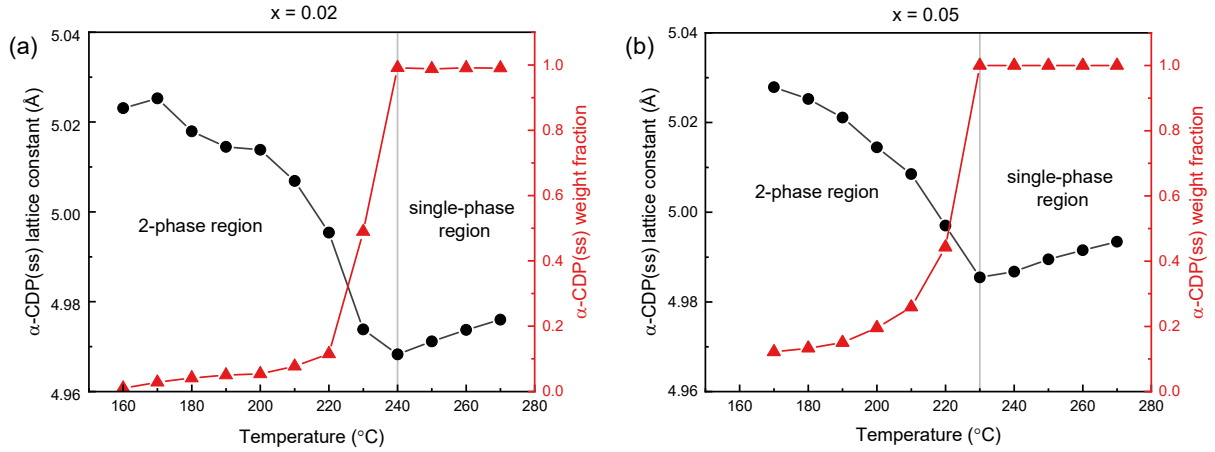

Figure S10. Continued.

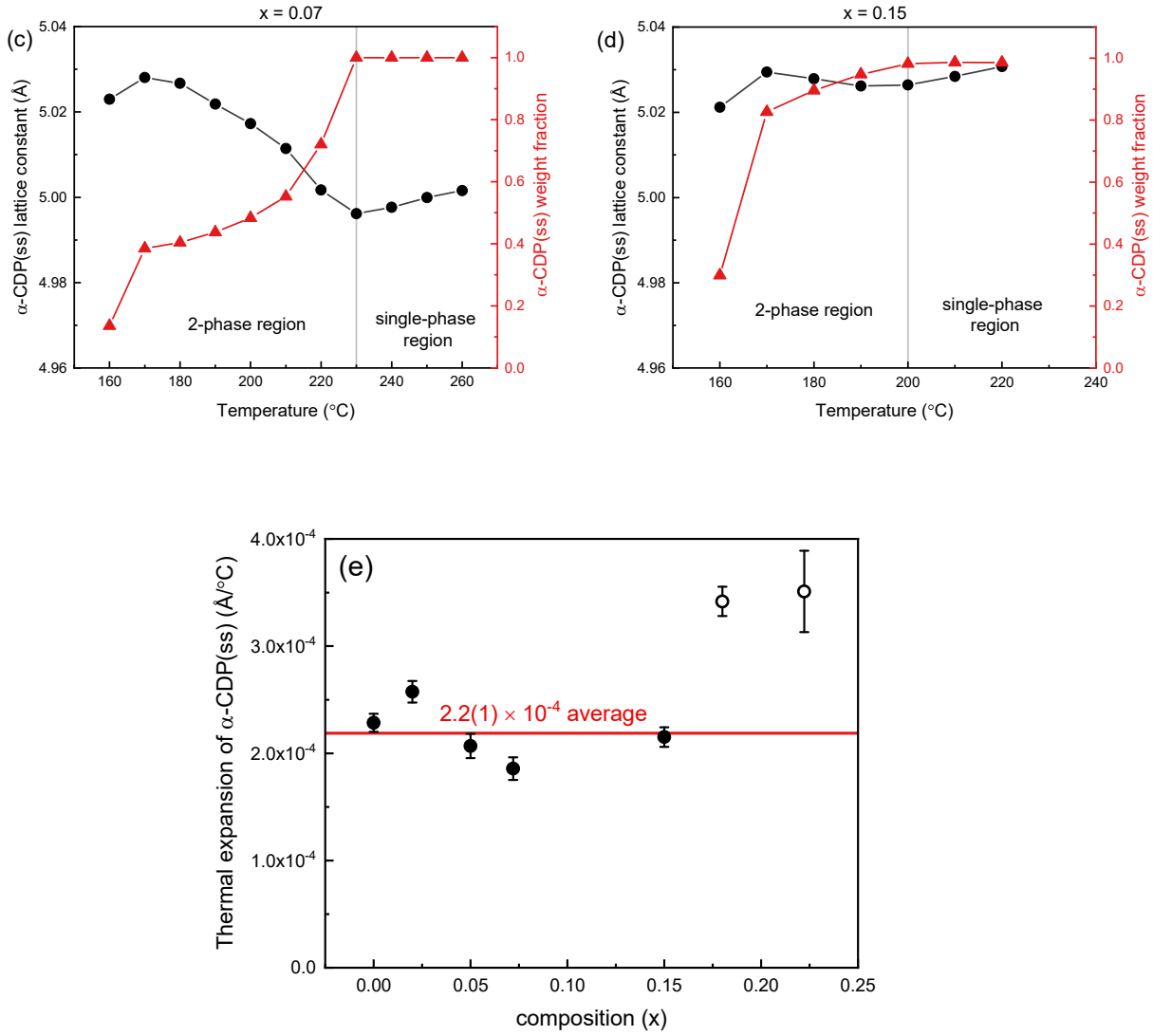

x = 0 (CsH_2PO_4) [See Figure 7a, main text for accompanying figure]

Temperature (°C)	α-CDP *a* (Å)	R_{wp}
232	4.9653(2)	11.96036
234	4.9652(2)	12.96135
236	4.9653(2)	14.13596
238	4.9654(1)	14.97225
240	4.9655(1)	15.75314
242	4.9659(1)	16.0244
244	4.9662(1)	15.96522
250	4.9675(2)	16.05989
260	4.9700(1)	15.5905

Figure S10. Continued

$x = 0.02$

Temperature (°C)	α-CDP *a* (Å)	Phase wt. fraction	R_{wp}, %
160	5.023(9)	0.010(5)	19.24
170	5.025(4)	0.028(3)	19.46
180	5.018(3)	0.041(4)	20.57
190	5.014(2)	0.050(5)	20.55
200	5.014(3)	0.054(5)	20.35
210	5.007(2)	0.077(5)	20.32
220	4.995(1)	0.115(6)	19.57
230	4.9738(4)	0.490(8)	19.36
240	4.9683(2)	0.992(5)	15.83
250	4.9712(2)	0.988(5)	15.99
260	4.9737(2)	0.991(5)	15.54
270	4.9760(2)	0.990(5)	15.21

$x = 0.05$

Temperature (°C)	α-CDP *a* (Å)	Phase wt. fraction	R_{wp}
170	5.0279(4)	0.121(4)	15.05
180	5.0252(4)	0.133(3)	15.54
190	5.0211(4)	0.150(3)	15.92
200	5.0145(3)	0.196(4)	15.83
210	5.0085(3)	0.259(4)	16.76
220	4.9970(3)	0.443(5)	17.12
230	4.9855(2)	1	19.40
240	4.9868(2)	1	19.54
250	4.9895(2)	1	19.92
260	4.9915(1)	1	14.89
270	4.9934(1)	1	13.78

$x = 0.07$

Temperature (°C)	α-CDP *a* (Å)	Phase wt. fraction	R_{wp}
160	5.023(1)	0.14(1)	20.46
170	5.0281(4)	0.385(8)	18.63
180	5.0267(4)	0.40(2)	18.02
190	5.0218(4)	0.437(7)	18.27
200	5.0172(4)	0.483(7)	17.92
210	5.0114(4)	0.552(8)	18.55
220	5.0017(4)	0.721(8)	20.63
230	4.9961(3)	1	19.62
240	4.9976(3)	1	19.63
250	4.9999(3)	1	20.24
260	5.0016(3)	1	19.90

Figure S10. Continued

$x = 0.15$

Temperature (°C)	α-CDP *a* (Å)	Phase wt. fraction	R_{wp}
160	5.0212	0.30(1)	14.67
170	5.0295(2)	0.83(1)	13.16
180	5.0279(2)	0.896(4)	12.49
190	5.0262(2)	0.947(4)	12.03
200	5.0264(2)	0.982(4)	12.21
210	5.0284(2)	0.986(4)	13.57
220	5.0307(3)	0.986(6)	16.65

Figure S11. Physical characteristics of samples of various compositions in the (1-*x*)CsH_2PO_4-*x*H_3PO_4 system, as indicated, as a function of temperature and steam partial pressure: (a), (b) mass and (c) lattice parameter of α-CDP(ss) for global compositions indicated. Despite mass sensitivity to steam partial pressure, the cell parameters of the α-CDP(ss) phase are unchanged in the two-phase regime of composition-induced thermal contraction. Lattice parameters in (c) were obtained by Rietveld refinement following the methodology reported above in the description of Figure S10 and full details of the refinement results under pH_2O = 0.65 atm are also reported with that figure. Details for pH_2O = 0.4 atm are reported here.

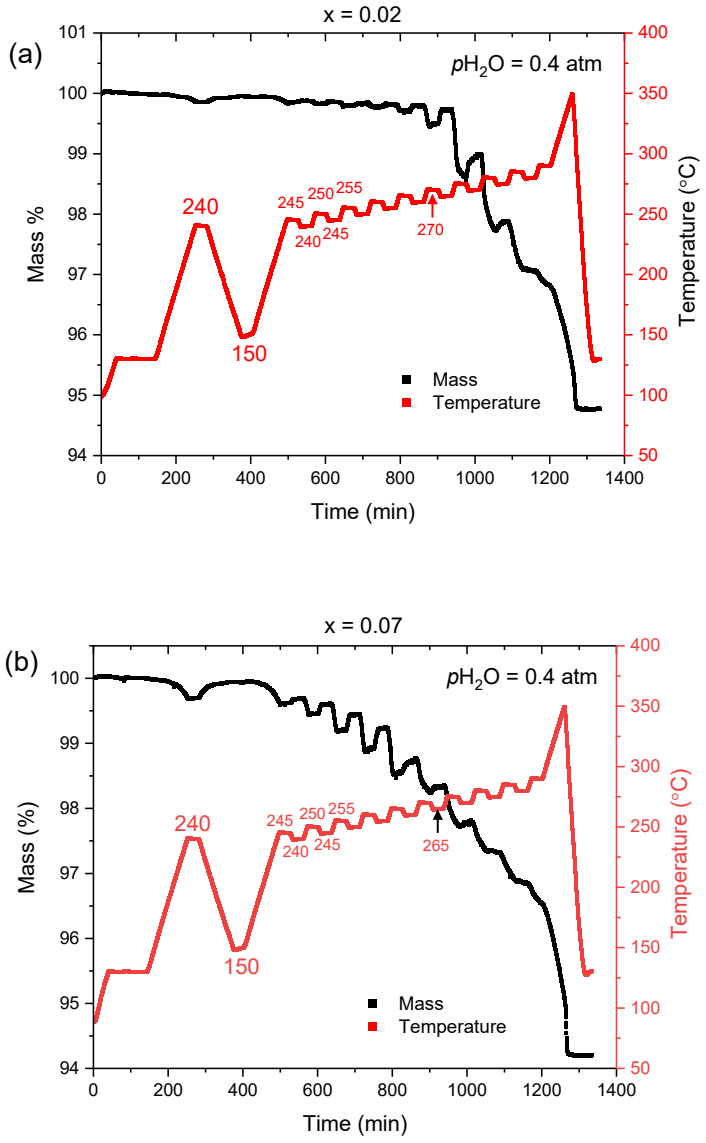

Figure S11. Continued

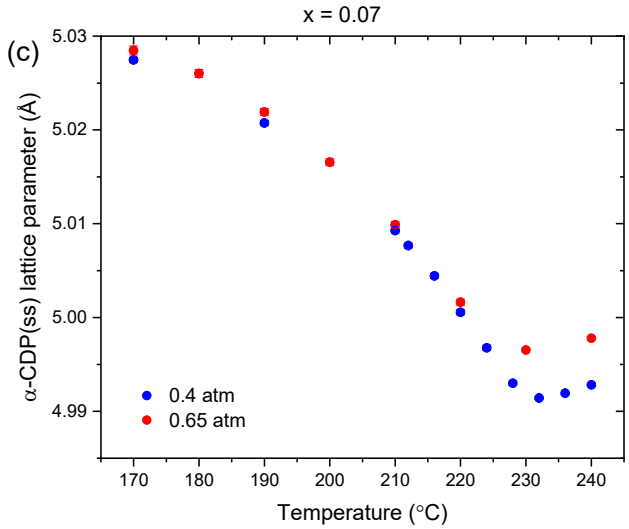

$x = 0.07$, $pH_2O = 0.4$ atm.

Temperature (°C)	α-CDP *a* (Å)	R_{wp}, %
170	5.0275(3)	12.58
190	5.0207(3)	12.29
210	5.0093(3)	10.98
212	5.0077(3)	11.07
216	5.0044(3)	11.62
220	5.0006(3)	11.36
224	4.9968(3)	11.90
228	4.9930(2)	11.29
232	4.9914(1)	11.66
236	4.9919(1)	12.25
240	4.9928(2)	12.55

Figure S12. Evaluation of the solvus phase boundary by diffraction analysis: (a) determination of the phase fraction of α-CDP(ss) as a function of composition, used for establishing the boundary by the Lever Rule, and (b) comparison of boundary determination by Vegard's Law (main text), the Lever Rule from part (a), and observation of the temperature at which CDP(m) is no longer detected in the diffraction data. As would be expected, the three approaches are in general agreement. The uncertainty is smaller from the Vegard's Law analysis than the Lever Rule analysis as a result of the difficulty of accurately establishing phase fractions from the diffraction data. Data plotted in (a) correspond to tabular listed provided in Figure S10.

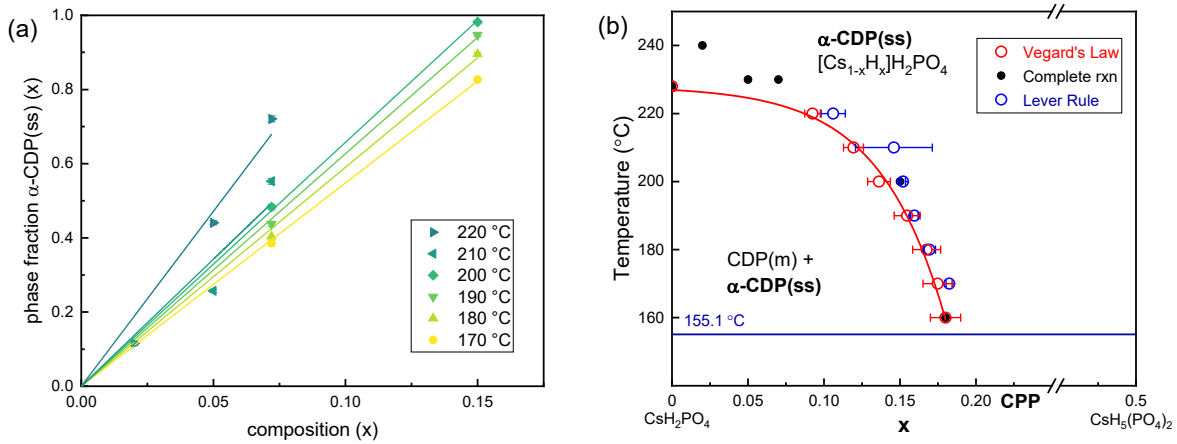

Figure S13. Conductivity of materials in the (1-*x*)CsH_2PO_4 – *x*H_3PO_4 system as a function of temperature on cooling with compositions as indicated. The data are consistent with that measured on heating with a slight hysteresis observed in the temperature of the reverse eutectoid reaction (α-CDP(ss) → CDP(m) + CPP).

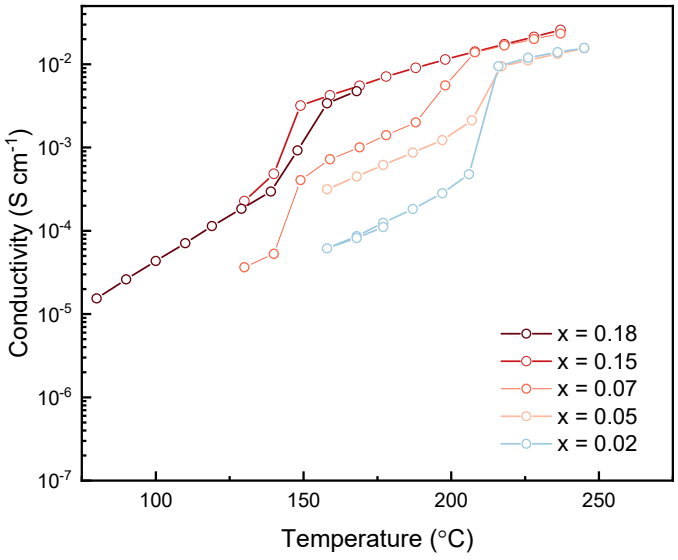

References

(1) Matsunaga, H.; Itoh, K.; Nakamura, E. X-ray Structural Study of Ferroelectric Cesium Dihydrogen Phosphate at Room Temperature. *J. Phys. Soc. Jpn.* **1980**, *48*, 2011-2014.

(2) Efremov, V. A.; Trunov, V. K.; Matsichek, I.; Gudinitsa, E. N.; Fakeev, A. A. Non-Equivalence of H-Atoms in $CsH_5(PO_4)_2$ Crystals. *Zhurnal Neorg. Khimii* **1981**, *26*, 3213-3216.

(3) Wang, L. S.; Patel, S. V.; Sanghvi, S. S.; Hu, Y. Y.; Haile, S. M. Structure and Properties of $Cs_7(H_4PO_4)(H_2PO_4)_8$: A New Superprotonic Solid Acid Featuring the Unusual Polycation $(H_4PO_4)^+$. *J. Am. Chem. Soc.* **2020**, *142*, 19992-20001.

(4) Yamada, K.; Sagara, T.; Yamane, Y.; Ohki, H.; Okuda, T. Superprotonic conductor CsH_2PO_4 studied by H-1, P-31 NMR and X-ray diffraction. *Solid State Ion.* **2004**, *175*, 557-562.